J Mater Sci: Mater Electron (2012) 23:1367–1372
DOI 10.1007/s10854-011-0600-x

Reactive templated grain growth and anisotropic electrical properties of $(Na_{0.5}K_{0.5})NbO_3$ ceramics without sintering aids

Danya Lv · Ruzhong Zuo · Shi Su

Received: 17 October 2011 / Accepted: 12 December 2011 / Published online: 21 December 2011

Abstract $(Na_{0.5}K_{0.5})NbO_3$ (KNN) ceramics with {100} orientation without sintering aids were fabricated by a conventional process and reactive templated grain growth using tabular $NaNbO_3$ template particles. The KNN specimen sintered at 1,170 °C for 15 h were found to have a relative density of 95.6%. The experimental results show that the textured ceramics have a pseudo-cubic {100} orientation degree of 96.2% and a microstructure with brick-like grains aligning in the direction parallel to the casting plane. The dielectric constant is much higher than the value for non-textured ceramics. Transition temperatures (T_{o-t}, T_c) are reduced and dielectric peaks are greater breadth. Remanent polarization P_r decreased from 19.40 (the random KNN) to 13.77 (textured KNN) μC/cm^2. The textured ceramics show anisotropic electrical properties between different directions of textured KNN ceramics, and show a very high electromechanical coupling factor $k_p = 0.58$ and a high piezoelectric constant $d_{33} = 225$ pC/N, compared to the random counterparts ($k_p = 0.31$, $d_{33} =$ 115 pC/N).

1 Introduction

The (K,Na)NbO_3 (KNN) ceramics have considerable potential as piezoelectric lead-free alternatives to Pb(Zr,Ti)O_3 ceramics. However, the piezoelectric properties (piezoelectric constant $d_{33} = 80$–120 pC/N, and electromechanical coupling factor $k_p = 0.34$–0.40) [1] of pure KNN are inferior to those of lead-based materials. Therefore, to replace the Pb-contained piezoceramics, it has been thought that some techniques to enhance the piezoelectric performance must be needed. The electrical properties of KNN ceramics have been observably improved by composition designing [2–6], doping [7–11] or grain orientation methods [12–17]. Texture control of polycrystals is an important approach to improve the piezoelectric properties of lead free materials without drastically changing the composition of the ceramics. There have been several grain orientation methods, such as oriented consolidation of anisometric particles [18], templated grain growth (TGG) [16], reactive templated grain growth (RTGG) [12], directional solidification technology [19] and multilayer grain growth technology [4] and so on. Among these methods, (R)TGG proves to be suitable for a material with cubic symmetry, particularly for perovskite structure materials. Crystallographic texturing of polycrystalline ferroelectric ceramics, such as $Pb(Mg_{1/3}Nb_{2/3})O_3$–$PbTiO_3$ [20], $Pb(Mg_{1/3}Nb_{2/3})O_3$–Pb(Zr,Ti)O_3 [21], $Bi_{0.5}(Na,K)_{0.5}TiO_3$ [22], $Sr_{0.53}Ba_{0.47}Nb_2O_6$ [23], and (K,Na,Li)(Nb,Ta,Sb)O_3 [12], results in greatly enhanced piezoelectric properties that can reach ≥50% of single-crystal values [24].

Saito et al. showed that Li^+, Ta^{5+}, and Sb^{5+} substitutions in KNN, combined with {001} grain orientation produced by RTGG method using a mixed $NaNbO_3$ and $KNbO_3$ matrix, which result in room temperature d_{33} and k_p values comparable to those of PZT. In a later paper, the same group textured CuO-doped KNN [13] and investigated the effect of CuO on oriented grain growth and the microstructural development in this system. The values of d_{33} and k_p are 123 pC/N and 0.54, respectively, about 40% higher than those of randomly oriented ceramics. Subsequently, they synthesized polycrystalline platelike $KNbO_3$

D. Lv · R. Zuo (✉) · S. Su
Institute of Electro Ceramics & Devices, School of Materials Science and Engineering, Hefei University of Technology, Hefei 230009, People's Republic of China
e-mail: piezolab@hfut.edu.cn

[14] (or $NaNbO_3$ [15]) particles from $K_4Nb_6O_{17}$ precursor and fabricated textured KNN with 1 mol% CuO. The authors reported that the ceramics have {100} orientation degree of 39.7% (or 45.3%) and a d_{33} value of 68 pC/N. Those work has focused on RTGG processing using a mixed $NaNbO_3$ and $KNbO_3$ matrix. For TGG process, Chang et al. [16] textured {001}-oriented $(K_{0.5}Na_{0.5})(Nb_{0.97}Sb_{0.03})O_3$ ceramics using $NaNbO_3$ templates. Through substitution of Sb^{5+} for Nb^{5+} and {001} grain orientation, the values of d_{33} and k_p increased to 208–218 pC/N and 0.64, respectively. Subsequently, the same group textured a CuO-doped $(K_{0.476}Na_{0.524})NbO_3$ [17] using 1 mol [KNN − x mol% CuO ($x = 0$, 0.5, and 1.0)] matrix powder and 0.05 mol $NaNbO_3$ templates. A novel (to the KNN system) two-step sintering and annealing process combined with CuO doping was demonstrated to improve density and maximize texture quality in textured KNN ceramics. The best electromechanical properties ($k_p \approx 0.58$, $d_{33} \approx 146$ pC/N) were achieved in 1 mol% CuO-doped KNN with $f = 99\%$. Recently, they also textured $(K_{0.5}Na_{0.5})_{0.98}Li_{0.02}NbO_3$ (KNLN) and $(K_{0.5}Na_{0.5})(Nb_{0.85}Ta_{0.15})O_3$ (KNNT) ceramics [25]. Both materials showed high textured ($f = 98\%$ for KNLN and $f = 99\%$ for KNNT) and enhanced piezoelectric response compared with randomly oriented ceramics. Moreover, textured KNLN showed higher piezoelectric properties ($k_p = 0.63$, $d_{33} \approx 192$ pC/N) than textured KNNT. However, RTGG or TGG studies in other perovskite systems suggest that better performance can be obtained in pure KNN. Additionally, CuO was used as an effective liquid-phase sintering aid doped in textured $(K_{0.5}Na_{0.5})NbO_3$ ceramics. CuO acting as an acceptor dopant in KNN can reduce piezoelectric properties which discovered in conventional solid state sintering method [26].

In this paper, we first textured KNN ceramics without sintering aids by RTGG method using {100}-oriented $NaNbO_3$ templates. These templates can be readily synthesized by topochemical microcrystal conversion (TMC) and are compositionally compatible with KNN. The platelike $NaNbO_3$ particles act as templates and also act as reactant composition for texturing ceramics. Then, we circumstantiate the effect of texture on the dielectric, ferroelectric and piezoelectric properties. Finally, we contrasted the electric properties of textured KNN ceramics in the perpendicular-cuts to give prominence to anisotropic electrical properties of KNN ceramics.

2 Experimental procedure

Platelike $NaNbO_3$ template particles were prepared by the TMC process. $Bi_{2.5}Na_{3.5}Nb_5O_{18}$(BiNN5) precursor particles of 0.5–1 μm in thickness by about 10–20 μm in length were synthesized from a mixture of Bi_2O_3 (99%), Na_2CO_3 (99.5%), and Nb_2O_5 (99.9%) at 1,140 °C for 3 h using the equal qualities of molten NaCl (>99.5%) salt as a flux (Fig. 1a). Heating a mixture of BiNN5 and Na_2CO_3 at 950 °C for 3 h in a NaCl flux, the platelike $NaNbO_3$ template particles were synthesized by TMC. The tabular $NaNbO_3$ template particle was found to have a morphology similar to the BiNN5 starting material: particles were about 0.5–1 μm in thickness by about 15–25 μm in length (Fig. 1b).

Using TMC-synthesized polycrystalline platelike $NaNbO_3$ particles as a template reactant, textured KNN ceramics were fabricated by the reactive templated grain growth method (RTGG) according to the following equation (the volume percentage of $NaNbO_3$ particles is about 9.7 vol.%):

$$0.4\,NaNbO_3(\text{matrix}) + 0.1\,NaNbO_3(\text{template}) + 0.5\,KNbO_3(\text{matrix}) \rightarrow KNN$$

The equiaxed $NaNbO_3$ and $KNbO_3$ particles were prepared from Na_2CO_3 and Nb_2O_5 or K_2CO_3 and Nb_2O_5 by heating twice at 750 °C for 3 h, respectively. The

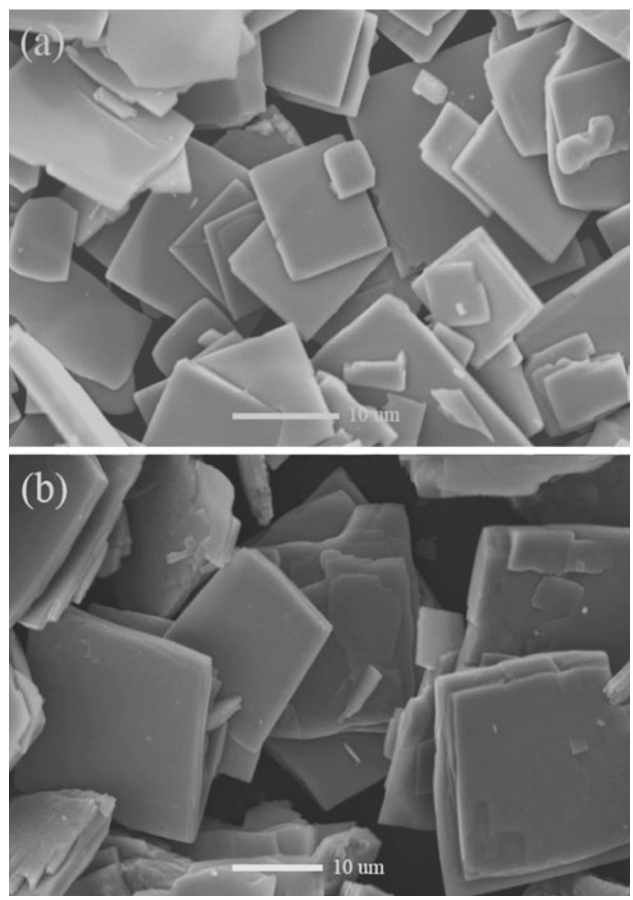

Fig. 1 SEM of **a** BiNN5 template precursor particles and **b** $NaNbO_3$ template particles synthesized by the TMC process

matrix and templates reactant were mixed, tape-cast, stacked and laminated to fabricate green compacts. After removing organic substances prior from the green compacts by heating at 600 °C for 10 h in air. The textured KNN polycrystal was prepared by sintering at 1,170 °C for 15 h in air. The compacts were further cut into tabular which the surfaces by polishing were perpendicular to the tape-casting plane.

A polished surface, parallel to the tape-casting plane and the pseudo-cubic Lotgering factor $F_{\{001\}}$ were detected at room temperature by an X-ray diffractometer (XRD, D/Max-RB, Rigaku, Tokyo, Japan) using a Cu Kα1 radiation on the polished sample surfaces. The microstructure on the cross-sectional perpendicular to the tape-casting plane was observed with a scanning electron microscope (SEM, JEOL6301F, Tokyo, Japan). Before SEM observation, the fractured surface was polished and etched by heating at 1,070 °C for 30 min. Dielectric properties were measured as a function of temperature by an LCR meter (HP 4980A, Agilent, USA) at 10 kHz. Polarization versus electric field hysteresis loops were measured by applying an electric field of triangular waveform at a frequency of 100 mHz by means of a ferroelectric measuring system (Precision Workstation 2000, USA). For measuring piezoelectric and electromechanical properties, samples were poled in stirring silicone oil at 110 °C applying 2.5 kV/mm for 30 min, and then cooled in the electric field. The piezoelectric constant d_{33} was measured by a Belincourt-meter (YE2730A, Sinoceram, Yangzhou, China). The planar electromechanical coupling factor k_p was determined by a resonance-antiresonance method with an impedance analyzer (HP4192A, Hewlett-Packard, USA).

3 Results and discussions

Figure 2a and b shows the XRD patterns of the surfaces of non-textured and textured $(K_{0.5}Na_{0.5})NbO_3$ ceramics at 1,100 °C for 3 h by a conventional process and 1,170 °C for 15 h in air, respectively. Non-textured and textured KNN ceramics show the pure orthorhombic perovskite structure, as clearly seen from split (100) and (200) peaks. This means that solid solution between the $NaNbO_3$ template and the matrix occurs and the platelike $NaNbO_3$ particles act as reactant composition in the RTGG process. An XRD spectra of random orientation ceramic shows the highest intensity for the (101) peak (Fig. 2a). For textured KNN samples, the intensity of the (101) peak decreases and a strong increase of the {100} diffraction peak intensities was observed (Fig. 2b). This intensity variation indicates an increase in the pseudo-cubic {100} orientation. The calculated the Lotgering factor f of the {100} orientation in pseudo-cubic notatin is 96.2%. This indicates that polycrystalline plate likes particle also act as templates for texturing ceramics.

The microstructures of the non-textured and textured ceramics are shown in Fig. 3a, b, respectively. It can be seen that the textured ceramics give well-ordered brick-layer-like KNN grains, which elongate and align parallel to the tape casting direction, whereas the grains in non-textured ceramics exhibit non-uniform grain growth. The averaged grain size in textured ceramics is much larger than that of the maximum grain size in non-textured ceramics. The reason of the larger grain size in textured ceramics comes from higher sintering temperature. High sintering temperature promoted epitaxial growth of the desired phase on these oriented $NaNbO_3$ templates, which acts as a substrate for epitaxy and as a seed for "exaggerated" grain growth. The epitaxial growth led to the textured KNN grain coarsening. The more uniformed grain growth in textured ceramics could be attributed to a uniform distribution of the template particles in the green ceramic body, which was followed by the uniform nucleation of grain growth at each grain. This observation keeps consistency with the above XRD results. A relative density of the textured KNN ceramics is 95.6%, compared to the random counterpart (~96%), which is measured from the Archimedes method. Porous structure of textured ceramics can be mainly attributed to the high volume percentage of $NaNbO_3$ template particles.

Figure 4 shows the variation of the dielectric constant ε_r of the textured KNN ceramics and non-textured ceramics. The textured materials exhibit similar temperature dependencies of ε_r compared with the random ones, and the dielectric constant is much higher than the value for non-textured ceramics. The room temperature dielectric constant for the textured ceramics (~553) was higher than the randomly oriented ones (~359), as is expected. The

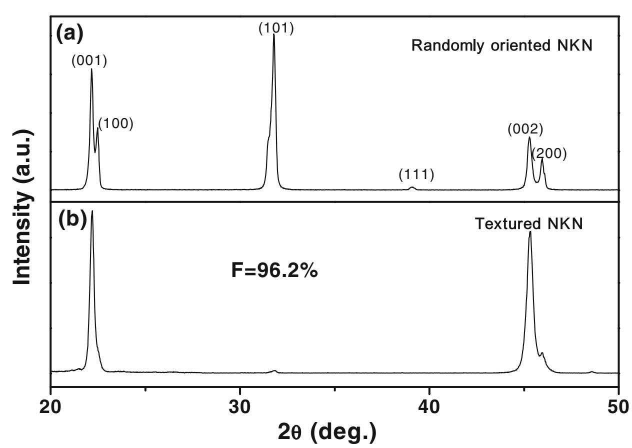

Fig. 2 The XRD patterns of the surfaces of (*a*) non-textured sintered at 1,100 °C for 3 h and (*b*) textured KNN sintered at 1,170 °C for 15 h in air

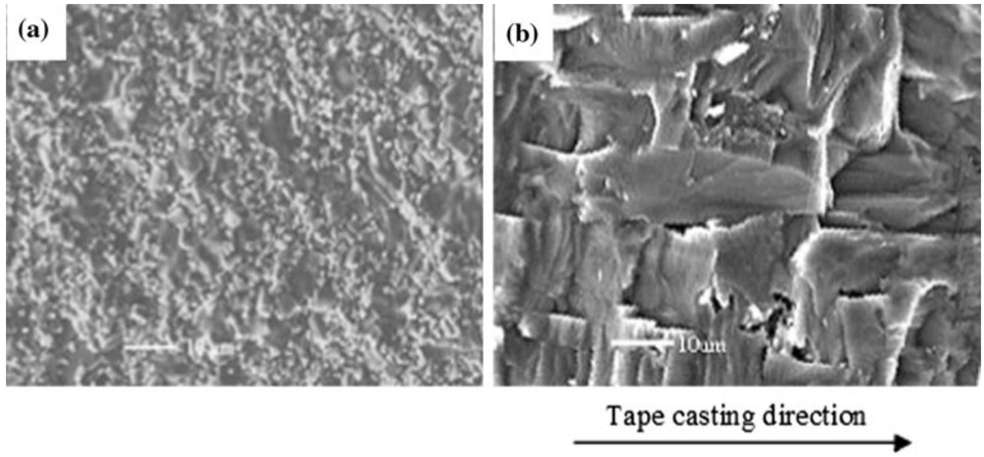

Fig. 3 The microstructures of **a** the non-textured KNN ceramic and **b** the textured KNN ceramic

maximum dielectric constant was $\varepsilon_{max} \approx 5{,}533$ for textured ceramics and $\varepsilon_{max} \approx 5{,}988$ for randomly oriented ceramics. The maximum dielectric constant of many orthorhombic perovskites occurs along the polarization direction [27]. So, for the textured ceramic, the maximum dielectric constant is located 45° away from the measurement direction, similar to the {100} oriented orthorhombic single case. However, for the randomly oriented ceramic, in which the pole density of maximum dielectric constant is equal in all directions, the averaging of the dielectric constant in all possible directions resulted in a lower dielectric constant than textured ceramics. They have two phase transitions at ~170 and ~383 °C, corresponding to the orthorhombic-tetragonal and tetragonal-cubic transitions, respectively. The lower of the transition temperature and the greater breadth of the dielectric peak may result from the internal stresses induced by the lattice mismatching during heating the crystal. Due to the high volatilization of potassium and sodium components in KNN, the obtained crystals were believed to be compositional non-uniformity. Thus, the K/Na ratio was slightly different in nano-regions and the compositional fluctuation lead to the lattice mismatching. It also shows very high anisotropy in the dielectric constant between the perpendicular-cuts and parallel-cuts samples. The textured ceramics parallel to the tape-casting plane exhibits dielectric constant much higher than the value for the perpendicular-cuts ones. This could be attributed to orientation of the plate like grain during tape casting.

P–E hysteresis loops of ceramics were recorded at room temperature and were shown in Fig. 5. After texturing, the remanent polarization P_r decreased from 19.40 to 13.77 μC/cm^2, and coercive field E_C increased from 8.6 to 10.3 V/cm. The orthorhombic KNN has statistically twelve possible polarization orientations along the pseudocubic {110}. Under the poling electric field, the dipoles switch as

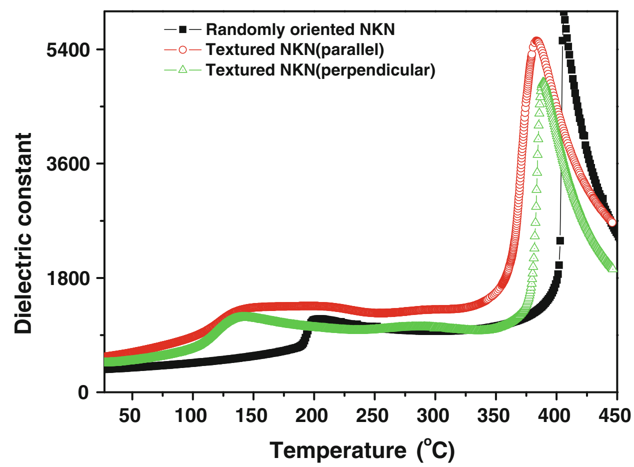

Fig. 4 The dielectric constant as a function of temperature for textured KNN ceramics sintered at 1,170 °C (10 kHz) and the non-textured KNN ceramics sintered at 1,100 °C (10 kHz)

much as possible along the electric field and occur as follows: for {100} poled, one four possible polar vectors along (110)\(−1−10), (101)\(−10−1), (1−10)\(−110) and (10−1)\(−101) are 45° with *E*-field and the other two polar vectors along (011) and (0−11) perpendicular to *E*-field. Therefore, for {100} oriented crystal has four possible polar vectors along (110)\(−1−10), (101)\(−10−1), (1−10)\(−110) and (10−1)\(−101). In randomly oriented ceramics, {100} is randomly distributed in 3-D space. For {001} textured orthorhombic ceramics, the angle between the measurement direction (texture direction) and polarization direction are 45° [28]. Therefore, due to the averaging of polarization of each domain in 3-D space, randomly oriented ceramics have a higher P_r than {100}-textured materials. It also shows very high anisotropy in *P–E* hysteresis loops between the perpendicular-cuts and parallel-cuts samples. The remnant polarization in the parallel-cuts is much higher than the P_r value (8.6 μC/cm^2) in the

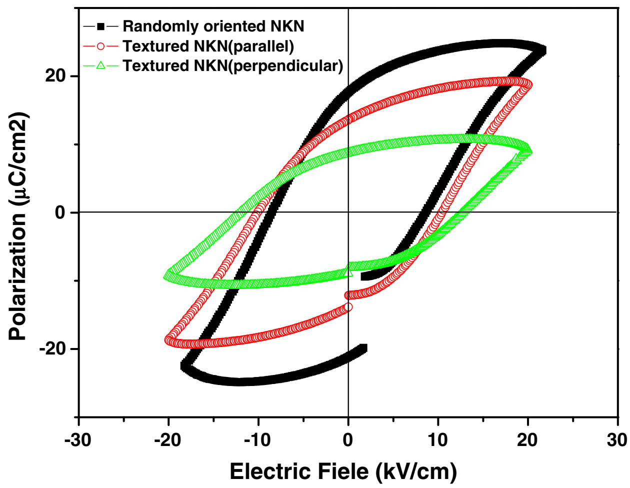

Fig. 5 Room temperature *P–E* hysteresis loops

perpendicular-cuts. In contrast, the coercive field E_C (10.3 kV/cm) of the parallel-cuts is lower than that of perpendicular-cuts (12.4 kV/cm).

The piezoelectric properties of the textured and non-textured ceramics are compared in Table 1. It can be seen that the piezoelectric coefficient d_{33} of the texture ceramic is 225 pC/N, and electromechanical coupling coefficient k_p is 0.58, which increase by about 96, 87%, respectively. The fixed angles between the measurement direction (texture direction) and polarization direction, result in a low driving force for domain wall movement. Consequently, piezoelectric properties are increasing. Additionally, when poling was done along {100} the polar direction is expected to incline close to the *E*-field in each domain, possibly resulting in increased orthorhombic lattice distortion. Although this distortion does not result in the structure transforming at room temperature, it actually has exerted an important influence on the ferroelectric (as shown in Fig. 5) and piezoelectric properties. The piezoelectric properties between the perpendicular-cuts and parallel-cuts samples show very high anisotropy. The piezoelectric properties of the perpendicular-cuts are considerable low.

Table 1 Piezoelectric properties of the textured and non-textured KNN ceramics

Piezoelectric properties	d_{33} (pC/N)	% Increase(comparing with non-textured)	k_p	% Increase(comparing with non-textured)
Non-textured	115	0	0.31	0
Textured (parallel direction)	225	96	0.58	87
Perpendicular direction	64	–	0.14	–

4 Conclusion

The results show that the textured ceramics have pseudo-cubic {001} orientation degrees of 96.2% and a microstructure with plated-like grains aligning in the direction parallel to the casting plane. After texturing, dielectric constant is much higher than the value for non-textured ceramics, transition temperatures ($T_{o\text{–}t}$, T_c) are reduced and dielectric peaks are greater breadth. Additionally, remanent polarization P_r decreased from 19.40 (the random KNN) to 13.77 (textured KNN) μC/cm^2. Textured KNN ceramics show very high electromechanical coupling factors $k_p = 0.58$ and high piezoelectric constants $d_{33} = 225$ pC/N, and show anisotropic electrical properties in the directions parallel and perpendicular to the casting plane.

Acknowledgments This work was financially supported by joint project of Chang-Shan-Jiao of Anhui Province (10140702014), a project of Natural Science Foundation of Anhui Province (1108085J14) and of China (50972035), and by a Program for New Century Excellent Talents in University, State Education Ministry (NCET-08-0766).

References

1. J. Rödel, W. Jo, K.T.P. Seifert, E.M. Anton, T. Granzow, J. Am. Ceram. Soc. **92**, 1153 (2009)
2. R.Z. Zuo, J. Fu, J. Am. Ceram. Soc. **94**, 1467 (2010)
3. Y.J. Dai, X.W. Zhang, G.Y. Zhou, Appl. Phys. Lett. **90**, 262903 (2007)
4. G.Z. Zang, J.F. Wang, H.C. Chen, W.B. Su, C.M. Wang, P. Qi, B.Q. Ming, J. Du, L.M. Zheng, Appl. Phys. Lett. **88**, 212908 (2006)
5. J.G. Wu, D.Q. Xiao, J. Appl. Phys. **102**, 114113 (2007)
6. D.M. Lin, K.W. Kwok, H.L.W. Chan, J. Phys. D Appl. Phys **40**, 6060 (2007)
7. R.Z. Zuo, J. Rödel, R.Z. Chen, L.T. Li, J. Am. Ceram. Soc. **89**, 2010 (2006)
8. D.M. Lin, M.S. Guo, K.H. Lam, K.W. Kwok, H.L.W. Chan, Smart Mater. Struct. **17**, 035002 (2008)
9. R.Z. Zuo, C. Ye, X.S. Fang, J. Am. Ceram. Soc. **91**, 914 (2008)
10. B. Malic, J. Bernard, J. Holc, D. Jenko, M. Kosec, J. Eur. Ceram. Soc. **25**, 2707 (2005)
11. Q. Chen, L. Chen, Q.S. Li, X. Yue, D.Q. Xiao, J.G. Zhu, X.L. Shi, Z.Q. Liu, J. Appl. Phys. **102**, 104109 (2007)
12. Y. Saito, H. Takao, T. Tani, T. Nonoyama, K. Takatori, T. Homma, T. Nagaya, M. Nakamura, Nature **432**, 84 (2004)
13. H. Takao, Y. Saito, Y. Aoki, K. Horibuchi, J. Am. Ceram. Soc. **89**, 1951 (2006)
14. Y. Saito, H. Takao, J. Eur. Ceram. Soc. **27**, 4085 (2007)
15. Y. Saito, H. Takao, J. Electroceram. **24**, 39 (2010)
16. Y.F. Chang, S.F. Poterala, Z.P. Yang, S. Trolier-Mckinstry, G.L. Messing, Appl. Phys. Lett. **95**, 232905 (2009)
17. Y.F. Chang, S.F. Poterala, Z.P. Yang, J. Mater. Res. **25**, 687 (2010)
18. T. Kimura, J. Ceram. Soc. Jpn. **114**, 15 (2006)
19. S.W. Sun, X.M. Pan, P.C. Wang, J. Appl. Phys. Lett. **84**, 574 (2004)
20. K.H. Brosnan, S.F. Poterala, R.J. Meyer, S. Misture, G.L. Messing, J. Am. Ceram. Soc. **92**, S133 (2009)

21. T. Richter, S. Denneler, C. Schuh, J. Am. Ceram. Soc. **91**, 929 (2008)
22. F. Gao, C.S. Zhang, X.C. Liu, L.H. Cheng, C.S. Tian, J. Eur. Ceram. Soc. **27**, 3453 (2007)
23. C. Duran, S. Trolier-McKinstry, G.L. Messing, J. Am. Ceram. Soc. **83**, 2203 (2000)
24. G.L. Messing, S. Trolier-McKinstry, E.M. Sabolsky, C. Duran, S. Kwon, B. Brahmaroutu, P. Park, H. Yilmaz, P.W. Rehrig, K.B. Eitel, E. Suvaci, M. Seabaugh, K.S. Oh, Crit. Rev. Solid State Mater. Sci. **29**, 45 (2004)
25. Y.F. Chang, S. Poterala, Z.P. Yang, G.L. Messing, J. Am. Ceram. Soc. **94**, 2494 (2011)
26. D.M. Lin, K.W. Kwok, H.L.W. Chan, J. Phys. D Appl. Phys. **41**, 045401 (2008)
27. K. Nakamura, Y. Kawamura, IEEE Trans. Ultrason. Ferroelectr. Freq. Control **47**, 750 (2000)
28. K. Nakamura, T. Tokiwa, Y. Kawamura, in *Proceedings of the 12th* IEEE *International Symposium on Applications of Ferroelectrics*, vol. 2 (2000), p. 717